Test particles in a magnetized conformastatic spacetime

Antonio C. Gutiérrez-Piñeres[1,2]⋆, Abraão J. S. Capistrano[3,4]† and Hernando Quevedo[1]‡

[1]*Instituto de Ciencias Nucleares, Universidad Nacional Autónoma de México, AP 70543, México, DF 04510, México*
[2]*Facultad de Ciencias Básicas, Universidad Tecnológica de Bolívar, Cartagena, 131001, Colombia*
[3]*Federal University of Latin-American Integration, 85867-670, P.o.b: 2123, Foz do iguassu-PR, Brazil*
[4]*Casimiro Montenegro Filho Astronomy Center, Itaipu Technological Park, 85867-900, Foz do Iguassu-PR, Brazil*

6 January 2016

ABSTRACT

A class of exact conformastatic solutions of the Einstein-Maxwell field equations is presented in which the gravitational and electromagnetic potentials are completely determined by a harmonic function. We derive the equations of motion for neutral and charged particles in a spacetime background characterized by this class of solutions. As an example, we focus on the analysis of a particular harmonic function which generates a singularity-free and asymptotically flat spacetime and, therefore, describes the gravitational field of a punctual mass endowed with a magnetic field. In this particular case, we investigate the main physical properties of equatorial circular orbits. We show that due to the electromagnetic interaction, it is possible to have charged test particles which stay at rest with respect to a static observer located at infinity. Additionally, we obtain an analytic expression for the perihelion advance of test particles. Our theoretical predictions are compared with the observational data calibrated with the ephemerides of the planets of the Solar system and the Moon (EPM2011). We show that, in general, the magnetic punctual mass predicts values that are in better agreement with observations than the values predicted in Einstein gravity alone.

Key words: Einstein-Maxwell equations – Exact solutions – Circular orbits – Perihelion advance.

1 INTRODUCTION

In recent years, the interest in studying magnetic fields has increased in both astrophysical and cosmological scales. In astrophysical dynamics, for instance, the study of disk sources for stationary axially symmetric spacetimes with magnetic fields is of special relevance mainly for the investigation of neutron stars, white dwarfs, and galaxy formation. In this context, usually, it is believed that electric fields do not have a clear astrophysical importance; nevertheless, there is a possibility that some galaxies are positively charged (González, Gutiérrez-Piñeres and Ospina, 2008; Bally and Harrison, 1978). On the other hand, magnetic fields are very common in astrophysical objects, and can drastically affect other physical properties (e.g, H-alpha emission, density mass, local shocks, etc.). For instance, magnetic fields in a galaxy can be measured from the non-thermal radio emission under the assumption of equipartition between the energies of the magnetic field and the relativistic particles (the so-called energy equipartition); this interaction can play an important role in the formation of arms in spiral galaxies (Krause, 2003). For nearby galaxies, one can use other effects such as optical polarization, polarized emission of clouds and dust grains, maser emissions, diffuse radio polarized emission and rotation measures of background polarization sources as well. In the case of the Milky Way, e.g., the magnetic field has been actively studied in its three main regions (central bulge, halo and accretion disk). Moreover, magnetic fields seem to play an important role in the formation of jets (resulting from collimated bipolar out flows of relativistic particles) and accretion disks near supermassive black holes (Zamaninasab et al., 2014).

It is important to stress that magnetic fields are found mainly in interstellar medium, remarkably, in spiral galaxies (Han, 2012) which can be described with a good approximation by means of thin disks. The magnetic and gravitational field of such objects can reach very high values, implying that a relativistic approach is necessary. In a series of recent works (Gutiérrez-Piñeres, 2015; Gutiérrez-Piñeres, Lopez-Monsalvo and Quevedo 2015; Gutiérrez-Piñeres and Capistrano, 2015 (a)), several classes of static and stationary axisymmetric exact solutions of the Einstein-Maxwell equations were derived which can be interpreted as describing the gravitational and magnetic fields

⋆ E-mail: gutierrezpac@gmail.com
† E-mail: abraao.capistrano@unila.edu.br
‡ E-mail: quevedo@nucleares.unam.mx

of static and rotating thin disks. Although these solutions satisfy the main theoretical conditions to be considered as physically meaningful, additional tests are necessary in order to establish their applicability in realistic scenarios. For instance, the study of the motion of test particles and the comparison of the resulting theoretical predictions with observations are essential to understand the physical properties of the solutions and the free parameters entering them. This is the main goal of the present work.

In this work, we follow the original terminology introduced by Synge (Synge, 1960), according to which conformastationary spacetimes are stationary spacetimes with a conformally flat space of orbits, and conformastatic spacetimes comprises the static subset. In a previous work (Gutiérrez-Piñeres and Capistrano, 2015 (b)), a static conformastatic solution of Einstein-Maxwell equations was presented and, in particular, the corresponding geodesic equations were derived explicitly. In the present work, we perform a detailed analysis of the equations of motion of test particles moving in a conformastatic spacetime which describes the gravitational and magnetic fields of a punctual source. In particular, we analyze the physical properties of circular orbits on the equatorial plane of the gravitational source. Additionally, we find an expression for the perihelion advance in a general magnetized conformastatic spacetime, and confront our theoretical results with the observational data calibrated with the EPM2011 ephemerides of the Solar System planets and the Moon.

This work is inspired on the approach presented in references (Pugliese, Quevedo and Ruffini (a), 2011) and (Pugliese, Quevedo and Ruffini (b), 2011). The analysis presented here serves as a "proof of principle" that gives a solid footing for a fuller study of particles motion in the field of relativistic disks and for a later study of in an ever more realistic astrophysical context.

This work is organized as follows. In Section 2, we present the Einstein-Maxwell equations for a conformastatic metric and show that there exists a class of solutions generated by harmonic functions. We derive the complete set of differential equations and first integrals that govern the dynamics of charged test particles moving in a conformastatic spacetime. In addition, we show that, due to the spacetime symmetries, the geodesic equations on the equatorial plane can be reduced to one single ordinary differential equation, describing the motion of a particle in an affective potential which depends on the radial coordinate only. In Section 3, we derive the explicit expressions for the energy and angular momentum of a particle moving along a circular orbit. In Section 4, we focus on the particular case of a punctual source. We analyze all the physical and stability properties of circular orbits along which charged test particles are moving. In Section 5, we obtain an expression for the perihelion advance of a charged test particle in a generic conformastatic spacetime in the presence of a magnetic field. In this section, we also illustrate our results by considering the case of a punctual source, and perform a comparison between our results, the results obtained in Einstein gravity alone, and the values observed for the secular perihelion precession of some inner planets and minor objects of the Solar System. Finally, in Section 6, we present the conclusions.

2   BASIC FRAMEWORK

In Einstein-Maxwell gravity theory, the background of a symmetric body can be described by the conformastatic metric in cylindrical coordinates ((Gutiérrez-Piñeres, González and Quevedo, 2013))

$$dS^2 = -c^2 e^{2\phi} dt^2 + e^{-2\phi}(dr^2 + dz^2 + r^2 d\varphi^2), \tag{1}$$

where c is the speed of light in vacuum and the metric potential ϕ depends only on the variables r and z. The field equations are the Einstein-Maxwell equations

$$R_{\alpha\beta} - \frac{1}{2}g_{\alpha\beta}R = k_0 E_{\alpha\beta}, \quad \nabla_\beta F^{\alpha\beta} = 0, \tag{2}$$

where $k_0 = 8\pi$ G c^{-4}. [1] The energy-momentum tensor $E_{\alpha\beta}$ is given by

$$E_{\alpha\beta} = \frac{1}{4\pi}\left\{F_{\alpha\gamma}F_\beta{}^\gamma - \frac{1}{4}g_{\alpha\beta}F_{\gamma\delta}F^{\gamma\delta}\right\},$$

where the electromagnetic tensor is denoted by $F_{\alpha\beta} = A_{\beta,\alpha} - A_{\alpha\beta}$, being $A_\alpha = (A_t, \mathbf{A})$ the electromagnetic four-potential. The components of the electromagnetic four-potential depend on r and z only.

To restrict ourselves to the case of an axially symmetric distribution on a magnetized background, we suppose that the only nonzero component of the four-potential is A_φ. Accordingly, Einstein-Maxwell equations (2) can be equivalently written as

$$\nabla^2\phi = \nabla\phi \cdot \nabla\phi, \tag{3}$$

$$\phi_{,r}^2 = \frac{G}{c^4 r^2}e^{2\phi}A_{\varphi,z}^2, \tag{4}$$

$$\phi_{,z}^2 = \frac{G}{c^4 r^2}e^{2\phi}A_{\varphi,r}^2, \tag{5}$$

$$\phi_{,r}\phi_{,z} = -\frac{G}{c^4 r^2}e^{2\phi}A_{\varphi,r}A_{\varphi,z}, \tag{6}$$

$$\nabla \cdot (r^{-2}e^{2\phi}\nabla A_\varphi) = 0, \tag{7}$$

where ∇ denotes the usual gradient operator in cylindrical coordinates, and a comma indicates partial differentiation with respect to the corresponding variable. The symmetry properties of the above differential equations allows us to reduce them to a single equation. In fact, by supposing a solution in the functional form $\phi = \phi[U(r,z)]$, where $U(r,z)$ is an arbitrary harmonic function restricted by the condition $U < 1$ for all r and z (Gutiérrez-Piñeres, González and Quevedo, (2013), Gutiérrez-Piñeres, (2015)), it is not difficult to prove that

$$\phi = -\ln(1-U), \quad A_\varphi(r,z) = \frac{c^2}{G^{1/2}}\int_0^r \tilde{r}U(\tilde{r},z)d\tilde{r}, \tag{8}$$

represent a solution of the system (3).

The electromagnetic field is pure magnetic which can be demonstrated by analyzing the electromagnetic invariant $\mathcal{F} = F^{\alpha\beta}F_{\alpha\beta}$, which in this case has the form

$$\mathcal{F} \equiv F^{\alpha\beta}F_{\alpha\beta} = \frac{2c^4(U_{,r}^2 + U_{,z}^2)}{G(1-U)^4} \geqslant 0. \tag{9}$$

---

[1] Along this work we use the CGS units such that $k_0 = 8\pi Gc^{-4} = 2,07 \times 10^{-48}$ s ^{2}cm^{-1}g^{-1}, $G = 6.674 \times 10^{-8}$cm^{3}g^{-1}s^{-2} and $c = 2.998 \times 10^{10}$ cm s^{-1}. Greek indices run from 1 to 4.

In fact, the nonzero components of the electromagnetic field are

$$B_r = \frac{c^2}{G^{1/2}} r U_{,r} \quad \text{and} \quad B_z = \frac{c^2}{G^{1/2}} r U_{,z} . \tag{10}$$

We conclude that any harmonic function $U(r,z) < 1$ can be used to construct an exact conformastatic solution of the Einstein-Maxwell equations. This is an interesting result which allows us to investigate the physical properties of concrete conformastatic spacetimes. Indeed, in the sections below we will investigate, as a particular example, one of the simplest harmonic solutions which turns out to describe the gravitational field of a punctual mass.

We now analyze the geodesic equations for a general case. The motion of a test particle of mass m and charge q moving in a conformastatic spacetime given by the line element (1) is described by the Lagrangian

$$\mathcal{L} = \frac{1}{2} m g_{\alpha\beta} \dot{x}^\alpha \dot{x}^\beta + \frac{q}{c} A_\alpha \dot{x}^\alpha, \tag{11}$$

where a dot represents differentiation with respect to the proper time. The equations of motion of the test particle can be derived from the Lagrangian (11) by using the Hamilton equations

$$\dot{p}_\alpha = -\frac{\partial \mathcal{H}}{\partial x^\alpha}, \quad \dot{x}_\alpha = \frac{\partial \mathcal{H}}{\partial p^\alpha},$$
$$\mathcal{H} = \dot{x}^\alpha p_\alpha - \mathcal{L} , \quad p_\alpha = \frac{\partial \mathcal{L}}{\partial \dot{x}^\alpha}, \tag{12}$$

where p_α and $\mathcal{H}$ are the momentum and Hamiltonian of the particle, respectively. The coupled differential equations (12) for the Lagrangian (11) are very difficult to solve directly by using an analytic approach. However, we can use the symmetry properties of the conformastatic field to find first integrals of the motion equations which reduce the number of independent equations. This is the approach we will use below.

Since the Lagrangian (11) does not depend explicitly on the variables t and φ, one can obtain the following two conserved quantities

$$p_t = -mc e^{2\phi} \dot{t} \equiv -\frac{E}{c}, \tag{13}$$

and

$$p_\varphi = mr^2 e^{-2\phi} \dot{\varphi} + \frac{q}{c} A_\varphi \equiv L, \tag{14}$$

where E and L are, respectively, the energy and the angular momentum of the particle as measured by an observer at rest at infinity. Furthermore, the momentum p_α of the particle can be normalized so that $g_{\alpha\beta} \dot{x}^\alpha \dot{x}^\beta = -\Sigma$. Accordingly, for the metric (1) we have

$$-c^2 e^{2\phi} \dot{t}^2 + e^{-2\phi}(\dot{r}^2 + \dot{z}^2 + r^2 \dot{\varphi}^2) = -\Sigma, \tag{15}$$

where $\Sigma = 0, c^2, -c^2$ for null, time-like and space-like curves, respectively.

The relations (13), (14) and (15) give us three linear differential equations, involving the four unknowns $\dot{x}^\alpha$. It is possible to study the motion of test particles with only these relations, if we limit ourselves to the particular case of equatorial trajectories, i. e. $z = 0$. Indeed, since the gravitational configuration is symmetric with respect to the equatorial plane, a particle with initial state $z = 0$ and $\dot{z} = 0$ will

remain confined to the equatorial plane which is, therefore, a geodesic plane. Substituting the conserved quantities (13) and (14) into Eq.(15), we find

$$\dot{r}^2 + \Phi = \frac{E^2}{m^2 c^2}, \tag{16}$$

where

$$\Phi(r) \equiv \frac{L^2}{m^2 r^2} \left(1 - \frac{q A_\varphi}{Lc}\right)^2 e^{4\phi} + \Sigma e^{2\phi} \tag{17}$$

is an effective potential. We assume the convention that the positive value of the energy corresponds to the positivity of the solution $E_\pm = \pm mc\Phi^{1/2}$. Consequently, $E_+ = -E_- = mc\Phi^{1/2}$.

3 CIRCULAR ORBITS

The motion of charged test particles is governed by the behavior of the effective potential (17). The radius of circular orbits and the corresponding values of the energy E and angular momentum L are given by the extrema of the function Φ. Therefore, the conditions for the occurrence of circular orbits are

$$\frac{d\Phi}{dr} = 0, \quad \Phi = \frac{E^2}{m^2 c^2}. \tag{18}$$

Thus, by calculating the condition (18) for the effective potential (17), we find the angular momentum of the particle in circular motion

$$L_{c\pm} = \frac{q A_\varphi}{c} + \frac{q r A_{\varphi,r} e^\phi \pm \sqrt{(q r A_{\varphi,r} e^\phi)^2 - 4\Sigma c^2 m^2 r^3 (2r\phi_{,r} - 1)}}{2c e^\phi (2r\phi_{,r} - 1)}. \tag{19}$$

Conventionally, we can associate the plus and minus signs in the subscript of the notation $L_{c\pm}$ to dextrorotation and levorotation, respectively.

Furthermore, by inserting the value of the angular momentum (19) into the second equation of Eq.(18), we obtain the energy $E^{(\pm)}_{c\pm}$ of the particle in a circular orbit as

$$E^{(\pm)}_{c\pm} = \pm mc e^\phi \left(\Sigma + \xi^{(\pm)}_c\right)^{1/2}, \tag{20}$$

where

$$\xi^{(\pm)}_c = \frac{\left[q r A_{\varphi,r} e^\phi \pm \sqrt{(q r A_{\varphi,r} e^\phi)^2 - 4\Sigma c^2 m^2 r^3 \phi_{,r} (2r\phi_{,r} - 1)}\right]^2}{4 m^2 c^2 r^2 (2r\phi_{,r} - 1)^2}. \tag{21}$$

Therefore, each sign of the value of the energy corresponds to two kind of motions (dextrorotation and levorotation) indicated in (20) and (21) by the superscripts $(\pm)$.

An interesting particular orbit is that one in which the particle is located at rest (r_r) as seen by an observer at infinity, i.e. $L = 0$. These orbits are therefore characterized by the conditions

$$L = 0, \quad \frac{d\Phi}{dr} = 0. \tag{22}$$

For the metric (1) these conditions give us the following

equation for the rest radius

$$\frac{2e^{2\phi}}{m^2 c^2 r^3}\left[q^2 A_\varphi\left(2rA_\varphi\phi_{,r}+rA_{\varphi,r}-A_\varphi\right)e^{2\phi}+\Sigma m^2 c^2 r^3\phi_{,r}\right]=0\,.$$
(23)

To find the value of the rest radius r_r, we must solve Eq.(23).

Notice that from Eqs. (23) and (20) it follows that if $e^{2\phi}=0$ for an orbit with a rest radius $r=r_r$, the energy of the particle is $E_r=0$. In the case $e^{2\phi}\neq 0$, we have

$$E^{(\pm)}_{r\pm}=\pm mce^{\phi}\left(\Sigma+\xi_r^{(\pm)}\right)^{1/2},$$
(24)

where

$$\xi^{(\pm)}_r=\frac{q^2 e^{2\phi}\left[rA_{\varphi,r}\pm\left(rA_{\varphi,r}+2A_\varphi\left(2r\phi_{,r}-1\right)\right)\right]^2}{4m^2 c^2 r^2\left(2r\phi_{,r}-1\right)^2}.$$
(25)

This analysis indicates that it is possible to have a test particle at rest with zero angular momentum ($L=0$) and non-zero energy ($E_r\neq 0$). This is a non-trivial effect that in the case of vanishing magnetic field has been associated with the existence of repulsive gravitational effects in Einstein gravity (Pugliese, Quevedo and Ruffini (a), 2011).

The minimum radius for a stable circular orbit corresponds to an inflection point of the effective potential function. Thus, we must solve the equation

$$\frac{d^2\Phi}{dr^2}=0,$$
(26)

under the condition that the angular momentum is given by Eq.(19). From Eqs.(18) and (26), we find that the radius and angular momentum of the last stable circular orbit are related by the following equations

$$\frac{2e^{4\phi}}{m^2 c^2 r^4}\Big[(Lc-qA_\varphi)^2\left(8r^2\phi_{,r}^2+2r^2\phi_{,rr}-8r\phi_{,r}+3\right)$$
$$+(Lc-qA_\varphi)\left(-8qr^2 A_{\varphi,r}\phi_{,r}-qr^2 A_{\varphi,rr}+4qrA_{\varphi,r}\right)$$
$$+q^2 r^2 A_{\varphi,r}^2 e^{2\phi}+2c^2\Sigma m^2 r^4\phi_{,r}^2+c^2\Sigma m^2 r^4\phi_{,rr}\Big]=0,\quad(27)$$

and

$$\frac{2e^{2\phi}}{m^2 c^2 r^3}\Big[e^{2\phi}(Lc-qA_\varphi)\Big((Lc-qA_\varphi)(2r\phi_{,r}-1)-qrA_{\varphi,r}\Big)$$
$$+\Sigma m^2 c^2 r^3\phi_{,r}\Big]=0.\quad(28)$$

It is possible to solve Eq.(28) with respect to the stable circular orbit radius which then becomes a function of the free parameter L. Alternatively, from Eq. (27) we find the expression

$$L_{lsco}^\pm = \frac{qA_\varphi}{c}+\Bigg\{qe^{\phi}\left(8r^2 A_{\varphi,r}\phi_{,r}^2+r^2 A_{\varphi,rr}-4rA_{\varphi,r}\right)$$
$$\pm\Bigg[q^2 e^{2\phi}\left(8r^2 A_{\varphi,r}\phi_{,r}^2+r^2 A_{\varphi,rr}-4rA_{\varphi,r}\right)^2$$
$$-4(q^2 r^2 A_{\varphi,r}^2 e^{2\phi}+2c^2\Sigma m^2 r^4\phi_{,r}^2+c^2\Sigma m^2 r^4\phi_{,rr})$$
$$\times(8r^2\phi_{,r}^2+2r^2\phi_{,rr}-8r\phi_{,r}+3)\Bigg]^{1/2}\Bigg\}$$
$$\times\left[2ce^{\phi}\left(8r^2\phi_{,r}^2+2r^2\phi_{,rr}-8r\phi_{,r}+3\right)\right]^{-1}\quad(29)$$

for the angular momentum of the last stable circular orbit.

Equation (29) can then be substituted in Eq. (28) to find the radius of the last stable circular orbit.

In this section, we found the expressions for the physical quantities which characterize the behavior of a charged test particle, moving along a circular trajectory in the gravitational field of a conformastatic mass distribution endowed with a magnetic field. These results are completely general, and can be applied to any solution of the corresponding Einstein-Maxwell equations.

4   THE FIELD OF A PUNCTUAL MASS IN EINSTEIN-MAXWELL GRAVITY

We now illustrate the results obtained in the precedent section, focusing on the main physical properties of test particles moving along circular orbits. As shown before, the class of harmonic conformastatic solutions is of particular interest, because all the metric components and the magnetic field are defined in terms of a single harmonic function. Let us consider one of the simplest harmonic functions which in Newtonian gravity would describe the gravitational field of a punctual mass, namely,

$$U(r,z)=-\frac{GM}{c^2 R},\quad R^2=r^2+z^2\,,$$
(30)

where M is a real constant. According to Eq.(8), for the metric and electromagnetic potentials we have

$$\phi(r,z)=-\ln\left(1+\frac{GM}{c^2 R}\right)\,,$$
(31)

and

$$A_\varphi(r,z)=\sqrt{G}M\left(1-\frac{z}{R}\right)\,,$$
(32)

respectively. At spatial infinity, the magnetic potential is non-zero and constant, except at the symmetry axis where it vanishes. Notice also that on the equatorial plane the magnetic potential is constant everywhere. As for the metric potential, its physical significance can be investigated by considering the asymptotic behavior of the metric component g_{tt} for which we obtain

$$\lim_{R\to\infty}g_{tt}(r,z)\approx -1+\frac{2GM}{c^2 R}-\frac{3G^2 M^2}{c^4 R^2}+\mathcal{O}\left(\frac{1}{R^3}\right)\,.$$
(33)

Accordingly, this particular solution can be interpreted as describing the gravitational field of a punctual mass on the background of a magnetic field. In the limiting case $M\to 0$, we obtain the Minkowski spacetime, indicating that M is the source of the gravitational and the magnetic field as well. This result can be corroborated by analyzing the Kretschmann scalar $\mathcal{K}=R_{\alpha\beta\gamma\delta}R^{\alpha\beta\gamma\delta}$ and the electromagnetic invariant $\mathcal{F}$ (see Eq.(9)) which in this case have the following expressions

$$\mathcal{K}=\frac{8M^2 c^8 G^2(G^2 M^2+6c^4 R^2)}{(c^2 R+GM)^8},$$
(34)

and

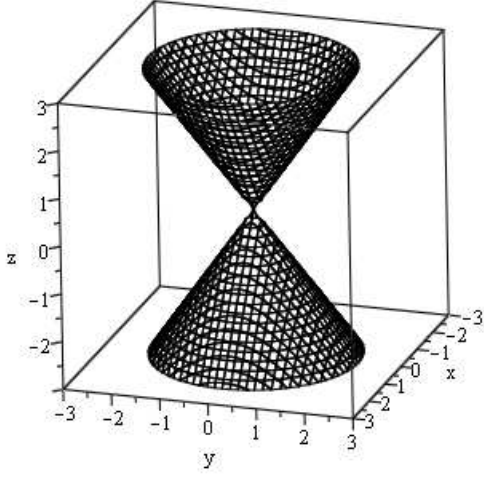$$\mathcal{F}=\frac{2GM^2 c^8}{(c^2 R+GM)^4},$$
(35)

Figure 1. Illustration of the spatial distribution of the magnetic lines of force of a punctual conformastatic source located at the origin of coordinates.

Figure 2. Angular momentum of a neutral test particle in terms of the radius orbit r_c/M.

respectively. In addition, from the expressions (33), (34) and (35), we conclude that the gravitational field is asymptotically Schwarzschild-like and singularity-free.

The field lines of the magnetic field are given by the ordinary differential equation $dr B_z = dz B_r$. Moreover, the nonzero components of the magnetic field are $B_r = G^{1/2} M r^2 R^{-3}$ and $B_z = G^{1/2} M r z R^{-3}$. Thus, we see that the equation

$$z^2 = \frac{(1-\alpha)^2}{\alpha(2-\alpha)} r^2 \ , \tag{36}$$

where $0 < \alpha < 2$, represents the lines of force of the magnetic field. The components of the magnetic field vanish at spatial infinity, and diverge at the origin $R = 0$. This, however, is not a true singularity as can be seen from the expression for the electromagnetic invariant (35). In Fig.1, we illustrate the spatial behavior of the lines of force of this magnetic configuration. It shows that the source of the magnetic field coincides with the punctual mass, in accordance with the analytic expressions for the gravitational and magnetic potentials.

4.1   Circular motion of a charged test particle

Consider the case of a charged particle moving in the conformastatic field of a punctual mass given by Eqs. (31) and (32). This means that we are considering the motion described by the following effective potential

$$\Phi(r) = \frac{c^6 r^2 (Lc - q\sqrt{G}M)^2}{m^2 (c^2 r + GM)^4} + \frac{\Sigma c^4 r^2}{(c^2 r + GM)^2}. \tag{37}$$

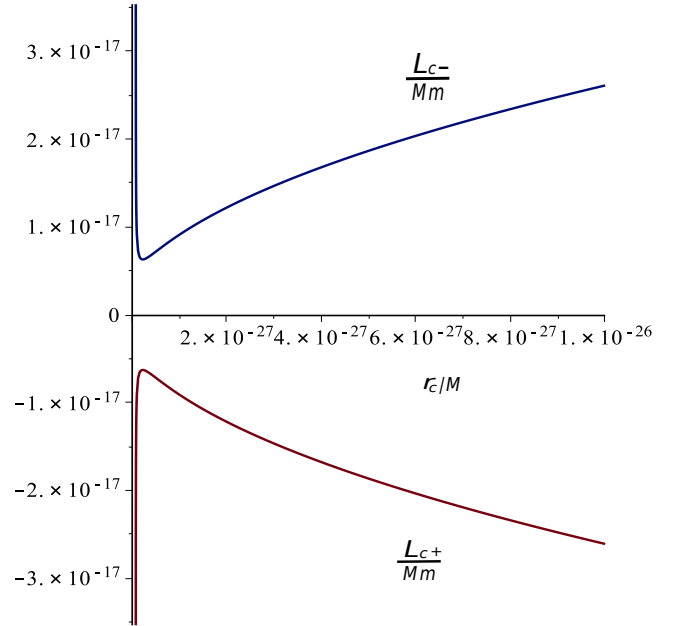We note that

$$e^{\phi(r)} = \frac{c^2 r}{c^2 r + GM} \tag{38}$$

on the equatorial plane.

According to the general results of the previous section, the angular momentum and the energy for a circular orbit with radius r_c are given by

$$L_{c\,\pm} = \frac{q\sqrt{G}M}{c} \mp \frac{(c^2 r_c + GM)m}{c^2} \sqrt{\frac{\Sigma GM}{c^2 r_c - GM}} \tag{39}$$

and

$$E_{c\,\pm} = \pm \frac{mc^4}{(c^2 r_c + GM)} \sqrt{\frac{\Sigma r_c^3}{c^2 r_c - GM}} \tag{40}$$

respectively. From Eqs.(39) and (40), we conclude that in order to have a time-like circular orbit the charged particle must be placed at a radius $r_c > GM/c^2$. In Fig.2, we illustrate the behavior of the angular momentum for the particular case of a neutral ($q = 0$) particle. We see that L_{c+} (L_{c-}) is always negative (positive) for all allowed values $r_c > GM/c^2$, and diverges in the limiting case $r_c = GM/c^2$. Since the charge q enters the angular momentum (39) as an additive constant, it does not affect the essential behavior of $L_{c\pm}$, but it only moves the curve along the vertical axis. However, the value of the effective charge q/m can always be chosen in such a way that either L_{c+} or L_{c-} become zero at a particular radius r_r. For instance, for L_{c+} to become zero, the charge q must be positive and greater than a certain value. This is the first indication that a circular orbit with zero angular momentum occurs as the result of the electromagnetic interaction.

As for the energy of circular orbits, we see from Eq.(40) that it does not depend explicitly on the value of the charge, but only on the radial distance from the central punctual mass. This, however, does not mean that the energy does not depend on the charge at all. Indeed, from Eq.(39) we see that, for a given angular momentum, the charge q influences the value of the circular orbit radius which, in turn, enters the expression for the energy. The behavior of the en-
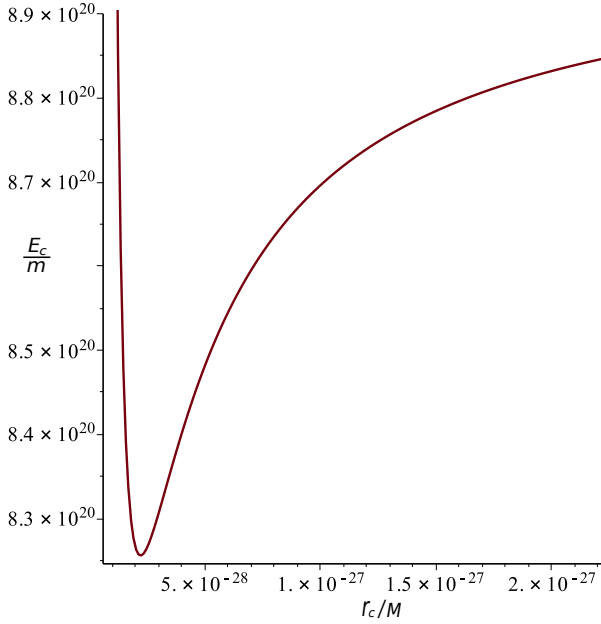
Figure 3. Energy of a charged test particle in terms of the radius orbit r_c/M.

Figure 4. Radii of the time-like orbits characterized by the conditions $L = 0$ and $d\Phi/dr = 0$ (see Eq.41). In this graphic the radii r_{r+}/M (solid curve) and r_{r-}/M (dashed curve) are plotted as functions of q/m.

ergy in terms of the radial distance is depicted in Fig.3. As the radius approaches the limiting value $r_c = GM/c^2$, the energy diverges indicating that a test particle cannot be situated on the minimum radius. The energy has an extremal located at the radius $r_c = 3GM/c^2$. We will see below that it corresponds to a particular orbit at which the particle stays at rest. At spatial infinity, we see that $E_{c+} \to mc^2$ which corresponds to the rest energy of the particle outside the influence of the magnetic and gravitational fields.

Let us now consider the conditions under the particle can remain at rest ($L = 0$) with respect to an observer at infinity. From Eq.(23) for $q \neq 0$ we find the trivial rest radius $r_r = 0$ for which the energy of the particle is $E_r = 0$. In addition, the non-trivial solution is given by the rest radii

$$\frac{r_{r\pm}}{M} = \frac{c^2 q^2 - 2\Sigma Gm^2 \pm \sqrt{c^2 q^2 (c^2 q^2 - 8\Sigma Gm^2)}}{2\Sigma m^2 c^2}. \quad (41)$$

The behavior of these radii is depicted in Fig.4. We can see that these solutions are physically realizable in the sense that the radii are always positive for all the allowed values of q/m. Indeed, the existence of a rest radius is restricted by the discriminant $q^2 - 8m^2 G$ in Eq.(41). For time-like test particles with $q^2/m^2 > 8G$, there exist an inner radius r_{r-} and an outer radius r_{r+} at which the particle can remain at rest. For the limiting value $q^2/m^2 = 8G$, the two radii coincide with $r_{r+} = r_{r-} = 3GM/c^2$. Instead, if $q^2/m^2 < 8G$, no radius exists at which the particle could stay at rest. Clearly, the existence of a rest radius is determined by the value of the test particle effective charge, indicating that a zero angular momentum orbit is the consequence of an electromagnetic effect due to the interaction of the test charge and the magnetic background.
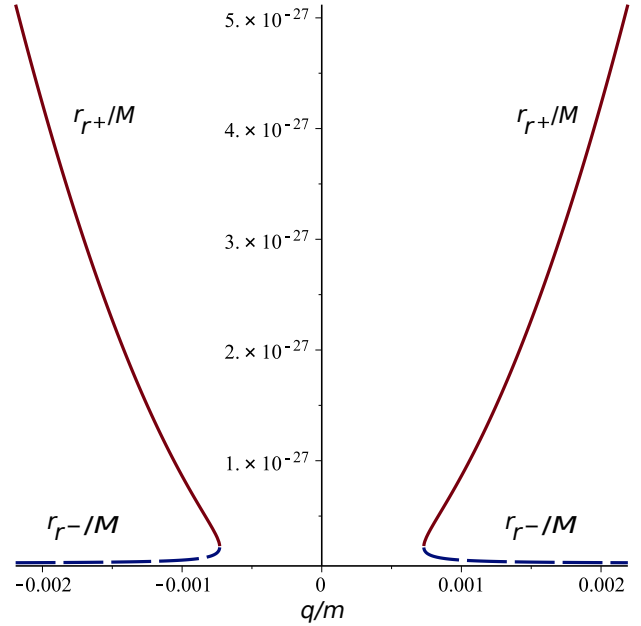
For the outer radius r_{r+} we have two possible positive

values of the corresponding energy, namely,

$$E_{r+}^{(\pm)} = +\frac{mc^2 \sqrt{2q^2 \left[q^2 - 2Gm^2 \pm \sqrt{q^2(q^2 - 8Gm^2)^2}\right]^3}}{\left[q^2 \pm \sqrt{q^2(q^2 - 8Gm^2)^2}\right]^2}, \quad (42)$$

whereas for the inner radius r_{r-} we two possible energies are always negative

$$E_{r-}^{(\pm)} = -E_{r+}^{(\pm)}. \quad (43)$$

In Fig.(5), we show the behavior of the energy at the outer rest radius. The minimum value of $\pm(3\sqrt{6}/8)mc^2$ is reached for $q^2 = 8Gm^2$, i.e., when the inner and outer radii coincide.

We now investigate the properties of the last stable circular orbit. According to Eq.(29), the angular momentum for this particular orbit must satisfy the relationship

$$L_{lsco\pm} = \frac{q\sqrt{G}M}{c} \pm \frac{(c^2 r + GM)m}{c^2}\sqrt{\frac{\Sigma GM(2c^2 r - GM)}{G^2 M^2 - 6c^2 GMr + 3c^4 r^2}}. \quad (44)$$

On the other hand, the angular momentum for any circular orbit is given by Eq.(39). Then, the comparison of Eqs.(44) and (39) yields the condition $r(c^2 r - 3GM) = 0$. Therefore, the radius of the last stable circular orbit is given by

$$r_{lsco} = \frac{3GM}{c^2}, \quad (45)$$

which, remarkably, does not depend on the value of the charge q. The corresponding angular momentum can be expressed as

$$L_{lsco\pm} = \frac{q\sqrt{G}M}{c} \pm \frac{2\sqrt{2\Sigma}GMm}{c^2}, \quad (46)$$
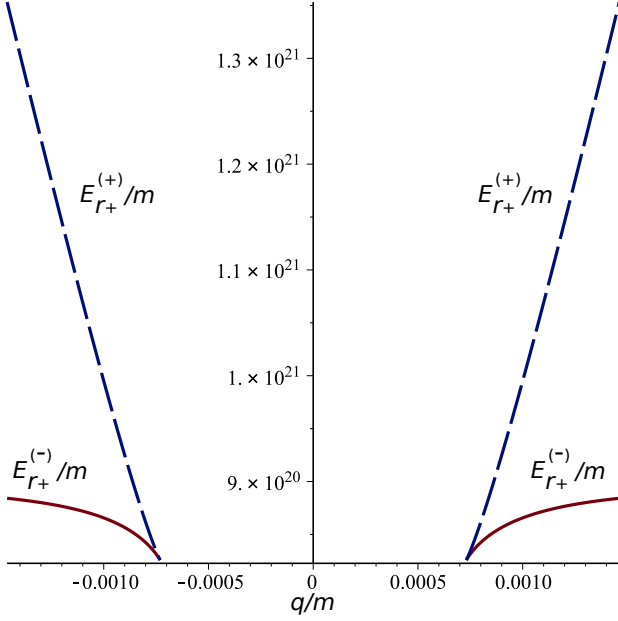
Figure 5. Energy of the charged particles for the time-like orbits characterized by the conditions $L = 0$ and $d\Phi/dr = 0$ (see Eqs.(42) and (43)). In this graphic the energy E_{r+}/m for the radius r_{r+}(solid curve) and E_{r+}/m for the radius r_{r-}(dashed curve) are plotted as functions of q/m.
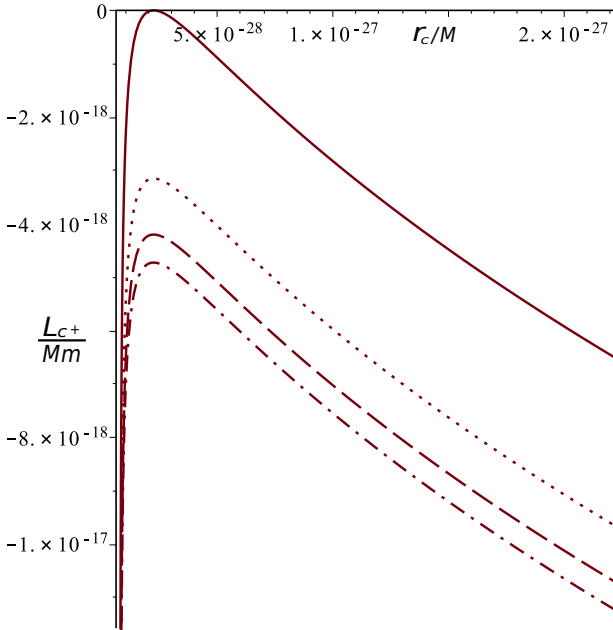

Figure 6. The angular momentum of the charged particles in a time-like circular orbit (see Eq. (39)). In this graphic the angular momentum L_c^+/Mm is plotted as a function of the radius r_c/M for some values of q/m is plotted. The continuous curve corresponds to the value $q/m = 2\sqrt{2G}$.
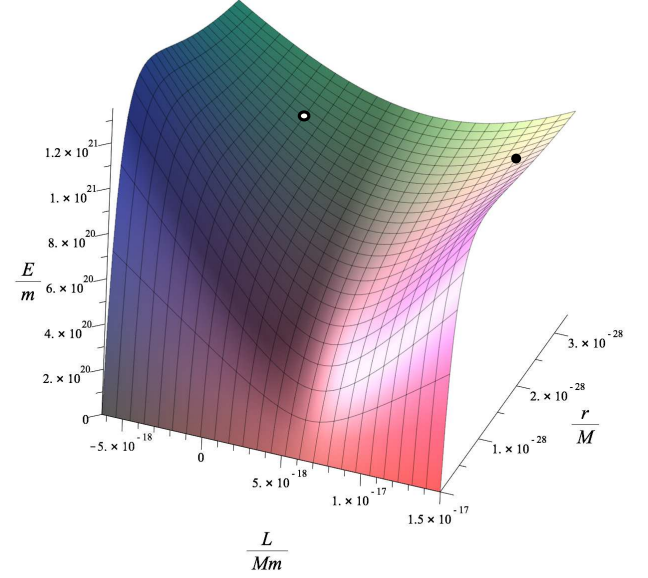

Figure 7. The energy of a particle with charge-to-mass-ratio $q/m = 2\sqrt{2G}$ is plotted as a function of r/M and the angular momentum L/Mm. Time-like circular orbits exist for $r/M > G/c^2$. The last stable circular orbit is represented by a black point ($r/M = 3G/c^2$, $L_{lsco+} = 4\sqrt{2}GMm/c$). The orbit with the same radius ($r/M = 3G/c^2$), but zero angular momentum ($L_{lsco-} = 0$) is represented by a white point.

and the energy reduces to

$$E_{lsco\,\pm} = \pm\frac{3}{4}\sqrt{\frac{3\Sigma}{2}}mc \ . \tag{47}$$

As we can see, the angular momentum depends explicitly on the value of the mass m and charge q of the test particle. Additionally, for space-like curves the angular momentum of the last stable circular orbit is not defined, whereas for a null curve it is $L_{lsco\,\pm} = q\sqrt{G}M/c$, and for a time-like particle it is $L_{lsco\,\pm} = (q\sqrt{G}\pm 2\sqrt{2}Gm)M/c$. Accordingly, if the charge of the particle is $q = 2\sqrt{2G}m$, then $L_{lsco-} = L_{c+} = L_r = 0$. Analogously, if $q = -2\sqrt{2G}m$, then $L_{lsco+} = L_{c-} = L_r = 0$.

Thus, we conclude that the last stable circular orbit occurs at the radius $r = 3GM/c^2$, independently of the value of the charge. Moreover, on the last stable orbit the particle is at rest, if the value of the charge is $q = \pm 2\sqrt{2G}m$ (see Fig. 6).

In Fig. 7, we present the general behavior of the energy function $E = \pm mc\sqrt{\Phi}$ in terms of the effective potential Φ given by Eq.(37). The branch corresponding to the positive energy of a particle with charge-to-masss-ratio $q/m = 2\sqrt{2G}$ is plotted as a function of r/M and the angular momentum L/Mm. We see that the effective potential (energy) tends to a constant at infinity. Since the radius for the last stable circular orbit is $r_{lsco} = 3GM/c^2$, for a particle with charge $q/m = 2\sqrt{2G}$ it is possible to stay at rest with $L_{lsco-} = 0$ (white point in Fig.7) or with angular momentum $L_{lsco+} = 4\sqrt{2}GMm/c$ (black point in Fig.7). A similar result is obtained if the charge is negative, corresponding to the angular momentum $-4\sqrt{2}G/c$ which indicates rotation in the counterclockwise direction.

It is worth noticing that a neutral particle cannot stay at rest with zero angular momentum. This can be deduced by replacing $q = 0$ in Eqs.(41), (42) and (43). In fact, with a zero value of q we obtain a negative rest radius. Finally, from Eqs.(45) and (46) we see that the last time-like stable circular orbit for neutral test particles can be placed at $r = 3GM/c^2$ with angular momentum $L_{lsco\,\pm} = \pm 2\sqrt{2}GMm/c$. Moreover, a neutral massless test particle can get $L = 0$ only at $r = 0$, as expected.

5 PERIHELION ADVANCE IN A CONFORMASTATIC MAGNETIZED SPACETIME

One of the most important tests of general relativity in astrophysics is the perihelion advance of celestial objects. In this section, we present the analytic expressions which determine the perihelion advance of charged test particle, moving in a conformastatic spacetime under the presence of a magnetic field. Starting from the first integral (15), we restrict the analysis to the motion of a particle on the plane with $z = 0$. Then, we have

$$\left(\frac{dr}{d\varphi}\right)^2 = -r^2\left[1 + \frac{m^2 r^2}{\left(L - \frac{q}{c}A_\varphi\right)^2}\left(\Sigma(1-U)^2 - \frac{E^2}{m^2 c^2}(1-U)^4\right)\right],$$
(48)

where all the quantities are evaluated at $z = 0$ and we have used the expressions for the energy and angular momentum of the particle given by Eqs.(13) and (14), respectively. With the change of variable $u = 1/r$, Eq.(48) can be transformed into

$$\frac{d^2 u}{d\varphi^2} + u^2 = F(u)$$
(49)

where

$$F(u) \equiv \frac{1}{2}\frac{dG}{du},$$
(50)

and

$$G(u) \equiv \frac{1}{\left(1 - \frac{qA_\varphi}{cL}\right)^2}\left[\frac{E^2}{c^2 L^2}(1-U)^4 - \frac{\Sigma m^2}{L^2}(1-U)^2\right].$$
(51)

Accordingly, by following the procedure proposed in (Harko, Kovács and Lobo, 2011), we have for the resulting perihelion advance

$$\delta\varphi = \pi\left(\frac{dF}{du}\right)_{u=u_0},$$
(52)

where u_0 is the radius of a nearly circular orbit, which is given by the roots of the equation $F(u_0) = u_0$.

5.1 Perihelion advance in the field of a punctual magnetized mass

In the previous subsection, we obtained an expression for the perihelion advance of a charged test particle in a generic conformastatic spacetime wiht a magnetic field. We now illustrate the results by considering a particular conformastatic

spacetime generated from the harmonic potential of a punctual mass

$$U(r,z) = -\frac{GM}{c^2 R}, \quad R^2 = r^2 + z^2.$$
(53)

Thus, by inserting Eq.(53) into Eq.(50) we obtain for $F(u)$

$$F(u) = \frac{\left[\frac{2E^2 GM}{c^4 L^2}\left(1 + \frac{GM}{c^2}u\right)^3 - \frac{\Sigma m^2 GM}{c^2 L^2}\left(1 + \frac{GM}{c^2}u\right)\right]}{\left(1 - \frac{q\sqrt{G}M}{cL}\right)^2}.$$
(54)

Accordingly, the perihelion advance of a particle in this spacetime is given by

$$\delta\varphi = \pi\frac{\left[\frac{6E^2 G^2 M^2}{c^6 L^2}x_0^2 - \frac{\Sigma m^2 G^2 M^2}{c^4 L^2}\right]}{\left(1 - \frac{q\sqrt{G}M}{cL}\right)^2},$$
(55)

where the term

$$x_0 \equiv 1 + \frac{GM}{c^2}u_0$$
(56)

satisfies the equation

$$2E^2 G^2 M^2 x_0^3 - \left[\Sigma m^2 G^2 M^2 c^2 + c^6 L^2\left(1 - \frac{q\sqrt{G}M}{cL}\right)^2\right]x_0$$
$$+ c^6 L^2\left(1 - \frac{q\sqrt{G}M}{cL}\right)^2 = 0.$$
(57)

Thus, by inserting the real solution of Eq.(57) into Eq.(54), we find that the perihelion advance of the test particle orbit is given by

$$\delta\varphi = \pi\frac{\psi_0 - k_2^2}{Q^2},$$
(58)

where

$$\psi_0 \equiv \frac{\left[6\left(Q^2 + k_2^2\right) + \left[54Q^2 k_1\left(-1 + \sqrt{1 - \frac{6\left(Q^2 + k_2^2\right)^3}{81Q^4 k_1^2}}\right)\right]^{2/3}\right]^2}{6\left[54Q^2 k_1\left(-1 + \sqrt{1 - \frac{6\left(Q^2 + k_2^2\right)^3}{81Q^4 k_1^2}}\right)\right]^{2/3}},$$

with

$$k_1^2 = \frac{E^2 G^2 M^2}{c^6 L^2}, \quad k_2^2 = \frac{\Sigma m^2 G^2 M^2}{c^4 L^2},$$

and also

$$Q^2 = \left(1 - \frac{q\sqrt{G}M}{cL}\right)^2.$$

Notice that when $q = 0$ (and, consequently $Q = 1$) we get the case in which Eq.(55) describes the perihelion advance of a neutral particle.

In order to get a real use of Eq.(58), we follow the procedure presented in (Harko, Kovács and Lobo, 2011). First, we rewrite both the angular momentum (19) and the energy (20), which depend on the radial distance r, in terms of the parameters that describe the orbit of rotating test particles. For the radial distance, one can use the ellipse formula in the Euclidean plane as

$$r = \frac{s(1 - \epsilon^2)}{1 + \epsilon\cos\varphi},$$
(59)

where s is the semimajor axis and ϵ the eccentricity of the

orbit. Moreover, we can rewrite Eq.(58) in terms of units related to observations as

$$\delta\varphi^\star = \pi\gamma^\star \frac{(\psi_0 - k_2^2)\, s^2}{Q^2 M_\odot T^2}, \tag{60}$$

where we have introduced the solar mass $M_\odot$ and the period T of the rotating body. The parameter $\gamma^\star = \frac{180/\pi}{3600}T$ allows us to transform units from radians to (secular) degrees. Since we have angular momentum and energy related to circular orbits, Eq.(60) still does not provide the observed secular drift of the perihelion. In order to obtain the real effective drift $\delta\varphi_{eff}$ and to alleviate the error propagation, we need to perturb Eq.(60) adding a "weighted" parameter that can measure the tiny shift of the orbit through time, which means, of course, that the perihelion $\delta\varphi$ advance has a time dependence. Thus, one can write the following variation to the secular time as

$$(\dot{\delta\varphi_{eff}}) = \left(\frac{\dot{\delta\varphi^\star}}{n}\right),$$

where n is the "weighted" parameter. As a result, one can take a direct integration and obtain the effective drift $\delta\varphi_{eff}$ as

$$\delta\varphi_{eff} = \frac{\delta\varphi^\star}{n} + n. \tag{61}$$

where the integration constant was conveniently set as the n parameter. Moreover, the values of n can be constrained by the observations from the solution of a simple squared polynomial equation such as

$$n = \pm\frac{1}{2}\left(\delta\varphi_{obs} \pm \sqrt{\delta\varphi_{obs}{}^2 - 4\delta\varphi^\star}\right). \tag{62}$$

where $\delta\varphi_{obs}$ is the observed secular shift.

When applied to the observational data based given in (Nambuya, 2010) and adding to it the supplementary precession corrections from EPM2011 (Pitjeva and Pitjev, 2013; Pitjev and Pitjeva, 2013), one can test Eq.(61). Thus, we obtain the results presented in table 1 for the perihelion precession of inner planets of the Solar system and two NEO's asteroids, 433 Eros and 3200 Phaethon. The data for the astrophysics parameters like semi-major axis, eccentricity, period and mass, can be found for planets in JPL solar system dynamics (http://ssd.jpl.nasa.gov/?planets) and for asteroids, in JPL small body database (http://ssd.jpl.nasa.gov/sbdb.cgi). The orbital periods used are in units of years.

As shown in table 1, the theoretical results match the observations. In fact, we see that the values predicted by the metric of the magnetized punctual mass match (in most cases) better the observational data than the values predicted in Einstein gravity. We conclude that the gravitational interaction generated by the magnetic field of the central body can play an important role in astrophysical observations.

In addition, some considerations must be noted. The constant Σ enters explicitly the expression for the perihelion advance (15), and it represents null, time-like and space-like curves. For $\Sigma = 0$, we do not have a solution since Eq.(61) diverges. For space-like trajectories, $\Sigma = -c^2$ no physical results are obtained, because in the corresponding Newtonian limit a differential equation is obtained, whose solution implies that r is negative. Moreover, no significant

Table 1. Comparison between the values for secular precession of inner planets in units of arcsec/century of the standard (Einstein) perihelion precession $\delta\phi_{eins}$ (Wilhelm and Dwivedi, 2014) for neutral test particles (planets and asteroids) in the conformastatic magnetized spacetime of a punctual mass $\delta\phi_{model}$. The data for $\delta\phi_{obs}$ stands for the secular observed perihelion precession in units of arcsec/century adapted from (Nambuya, 2010) by adding a supplementary precession correction from EPM2011 (Pitjeva and Pitjev, 2013; Pitjev and Pitjeva, 2013). In addition, the results for the NEOS 433 Eros and 3200 Phaethon are also presented.

Object	$\delta\phi_{obs}\ ('' .cy^{-1})$	$\delta\phi_{eins}('' .cy^{-1})$	$\delta\phi_{model}('' .cy^{-1})$
Mercury	43.098 ± 0.503	42.97817	43.10
Venus	8.026 ± 5.016	8.62409	8.040
Earth	5.00019 ± 1.00038	3.83848	5.044
Mars	1.36238 ± 0.000537	1.35086	1.730
433 Eros	1.60	1.57317	1.886
3200 Phaethon	10.1	10.1201	10.130

differences were found for different values of the charge of the order $q/m \sim 10^{-3}$, which is the value where the behavior of the energy and angular momentum becomes affected by the presence of the effective charge. In the same sense, no differences could be found when using both solutions for the angular momentum $L_{c\,\pm}$ and energy $E_{c\,\pm}$, indicating that the n parameter takes into account the differences between those solutions.

6 CONCLUSIONS

In this work we have shortly shown the characteristics of the motion of a charged particle along circular orbits in a spacetime described by a conformastatic solution of the Einstein-Maxwell equations. As a particular example we have considered the case of a charged particle moving in the gravitational field of a punctual source placed at the origin of coordinates. Our analysis is based on the study of the behavior of an effective potential that determines the position and stability properties of circular orbits. We have found that a classical radius $r = 3GMc^2$ of circular orbits exists with zero angular momentum. This phenomenon is interpreted as a consequence of the repulsive force generated by the charge distribution. Interestingly, we have found a spacetime with singularity-free which is not exclusive to the case of naked singularities. Moreover, we have obtained a region of stability determined by the angular momentum $L_{lsco}^\pm/Mm = q\sqrt{G}/(mc) + 2\sqrt{2}G/c$ and the radius $r = 3GMc^2$. It is worth noticing that a neutral particle can not be located at rest with angular momentum zero. We also notice that the last time-like stable circular orbit for neutral test particles with $m \neq 0$ can be placed at $r = 3GM/c^2$ with angular momentum $L_{lsco\,\pm} = \pm 2\sqrt{2}GMm/c$, and that neutral test particle massless only can get $L = 0$ when are placed at $r = 0$, as expected.

In addition, we have also calculated an expression for the perihelion advance of a test particle in a general magnetized conformastatic spacetime obtaining a good agreement

with the observed values for the perihelion of inner Solar planets and some selected NEO asteroids. It is worth noting that all results presented were obtained with the initial assumption of a neutral particle, in accordance with the fact that planets are largely neutral. Specifically, in the perihelion drift, we find that the differences between a neutral charge and a charged particle are sightly small, when realistic values for the effective charge are used. This means that the electromagnetic interaction between the charge and the central magnetized body does not seriously affect the value of the perihelion advance. Nevertheless, the magnetic field enters explicitly the metric components and, consequently, affects the motion of neutral test particles through the gravitational interaction. This explains why the numerical predictions of the perihelion advance generated by a punctual magnetized mass are (in most cases) in better agreement with observations than the predictions of Einstein's theory alone.

REFERENCES

Bally J., Harrison E.R, 1978, Astrophys. J., 220, 743.
Bicak J., Lynden-Bell D., Katz J., 1993, Phys. Rev. D, 47, 4334.
Bicak J., Lynden-Bell D., Pichon C., 1993, Mon. Not. R.Astron. Soc., 265, 126.
Binney J., Tremaine S., 2011, *Galactic dynamics*, Princeton University press.
Chakraborty K., Rahaman F., Ray S., Nandi A., Islam N., Gen.Rel.Grav., 10, 46, 1807.
Chamorro A., Gregory R., Stewart J.M., 1987, Proc. R. Soc. A 413, 251.
Chandrasekhar, Subrahmanyan, 1968, The mathematical theory of black hole, Vol 69, Oxford University Press.
González G.A., Gutiérrez-Piñeres A.C, Ospina P.A., 2008, Phys. Rev. D, 78, 064058.
González G.A., Letelier P.S., 1999, Class. Quant. Grav., 16, 479.
González G.A., Espitia O.A, 2003, Phys. Rev. D, 68, 104028.
Gutiérrez-Piñeres A.C., 2015, Gen. Rel. Grav., 47, 54.
Gutiérrez-Piñeres A.C., and Lopez-Monsalvo, C S and Quevedo, H 2015, Gen. Rel. Grav., 47, 144.
Gutiérrez-Piñeres A.C., González G.A., Quevedo H., 2013, Phys. Rev. D, 87, 044010.
Gutiérrez-Piñeres A.C. and Capistrano, Abraão J. S., 2015, arXiv:1510.05400.
Gutiérrez-Piñeres A.C. and Capistrano, Abraão J. S., 2015, Advances in Mathematical Physics, vol. 2015, Article ID 916026.
Han J., 2012, *Magnetic fields in our Milky Way Galaxy and nearby galaxies, Solar and Astrophysical dynamos and Magnetic Activity*, Proceedings IAU Symposium, 294, Eds.:A. G. Kosovichev, E. M. de Gouveia Dal Pino, Y. Yan.
Harko T., Kovács Z., Lobo F.S.N., 2011, Proc. R. Soc. A, 467, 2129, 1390.
Herrera L., Di Prisco A., Ibañez J., Ospino J., 2014, Phys. Rev. D, 89,8,084034.
Krause M., 2003, In: *The Magnetized Interstellar Medium*, Eds.: B. Uyanker, W. Reich, R. Wielebinski.
Letelier P.S., Oliveira S.R., 1987, J. Math. Phys., 28, 165.
Lemos J.P.S., 1989, Class. Quant. Grav., 6, 129.
Lynden-Bell D., Pineault S., 1978, Mon. Not. R. Astron. Soc., 185, 679.
Lynden-Bell D., Pineault S., 1978, Mon. Not. R. Astron. Soc., 185, 695.
Morgan T., Morgan L., 1969, Phys. Rev., 183, 1097.
Morgan L., Morgan T., 1970, Phys. Rev. D2, 2756.
Nambuya G.G., 2010, Mon. Not. R. Astron. Soc., 403, 1381.

Pitjeva E. V., Pitjev N.P., 2013, Mon. Not. R. Astron. Soc., 432, 4, 3431-3437.
Pitjev N. P., Pitjeva, E. V., 2013, Astron. Lett., 39, 3, 141-149.
Pugliese D., Quevedo H., Ruffini R., 2011, Phys. Rev. D, 83, 10, 104052, 26.
Pugliese D., Quevedo H., Ruffini R., 2011, Phys. Rev. D, 83,2, 024021, 12.
Stephani H., Kramer D., MacCallum M., Hoenselaers C., Herlt E., 2003, *Exact solutions of Einstein's field equations*, Cambridge University Press.
Synge J.L., 1960, *Relativity: the general theory. (Buch)*, North-Holland Pub. Co., Interscience Publishers.
Voorhees B.H., 1972, Phys. Rev. D, 5, 2413.
Wilhelm K., Dwivedi B. N., 2014, New Astronomy, 31, 51-55.
Zamaninasab M., Clausen-Brown E., Savolainen T., Tchekhovskoy A., 2014, Nature(letters), 126, 510.